Available online at www.sciencedirect.com
SCIENCE DIRECT®
Journal of Magnetic Resonance 169 (2004) 250–256
JMR Journal of Magnetic Resonance
www.elsevier.com/locate/jmr

Nanoscale NMR velocimetry by means of slowly diffusing tracer particles

Helena Wassenius[a,b,c,*] and Paul T. Callaghan[a]

[a] *MacDiarmid Institute for Advanced Materials and Nanotechnology, School of Chemical and Physical Sciences, Victoria University of Wellington, New Zealand*
[b] *Department of Materials and Surface Chemistry, Chalmers University of Technology, Göteborg S-412 96, Sweden*
[c] *BIM Kemi AB, Box 3102, Stenkullen S-443 03, Sweden*

Received 1 December 2003; revised 26 April 2004

Abstract

The resolution of NMR velocimetry is inherently limited by random displacements due to molecular self-diffusion, and has so far not extended below a few tens of microns. We report here an extension to the nanoscale domain, a result achieved by the use of slowly diffusing, NMR-visible core-shell latex particles. These particles comprise an oil core surrounded by a solid polymer shell, making spheres of diameter 370 nm. Using these particles in the annulus of a concentric cylinder Couette cell, we have measured flow-induced displacements down to a few hundreds of nanometers, allowing the observation of the solid-to-liquid transition of a glassy system. We envisage new possibilities for NMR velocimetry as an experimental tool for colloidal chemistry and physics.

Keywords: NMR velocimetry; Nanoscale; Core-shell latex; Couette; Yield stress

1. Introduction

Among the many achievements of magnetic resonance has been the measurement of fluid translational motion, first suggested by Hahn in his 1950 paper on Spin Echoes, and further elaborated by Carr and Purcell and by Stejskal and Tanner [1–3]. The potential for magnetic resonance to provide detailed insight regarding complex fluid motion was demonstrated by Hayward et al. [4], who showed that the precise distribution of fluid velocities present in a molecular ensemble could be measured using the pulsed magnetic field gradient spin echo (PGSE) technique. With the advent of magnetic resonance imaging, the mapping of fluid velocities became possible. NMR velocimetry is now an established technique in medicine, in chemical engineering, and in materials science [5–11]. It is precise and accurate, has good dynamic range, and it can probe optically opaque materials. While various modalities have been proposed as a means of providing flow contrast, the phase-encoding procedures associated with PGSE approaches have proven robust and information-rich, for example providing precise details of the distribution of displacements in the molecular ensemble. In particular, the capacity of PGSE NMR to measure molecular diffusion makes the technique particularly valuable. However, it is the existence of molecular self-diffusion that inherently limits the flow sensitivity of NMR velocimetry.

To image velocity we encode the signal with a pulsed gradient spin echo (PGSE) pair. These pulses define a wave vector domain, q, and impart a phase shift to the spins that depends directly on the motion of their parent molecules. (Note that q is the area under the gradient pulse, defined by $\gamma g\delta$, where g is the magnetogyric ratio, γ is the amplitude of the pulse, and δ its duration.) In particular, a spin moving by a displacement Z in the direction of the wave vector over the time Δ between the PGSE pulse pair acquires a phase factor $\exp(iqZ)$. Inverse Fourier transformation of the signal with respect to q returns, for each pixel of the image, the function, $\overline{P}_s(Z,\Delta)$, which describes the ensemble distribution of

* Corresponding author. Fax: +46-31-16-00-62.
E-mail address: hewa@surfchem.chalmers.se (H. Wassenius).

1090-7807/$ - see front matter © 2004 Elsevier Inc. All rights reserved.
doi:10.1016/j.jmr.2004.05.005

molecular displacements for that location. In general $\overline{P_s}(Z,\Delta)$ is given by [7]

$$\overline{P_s}(Z,\Delta) = A e^{-(v\Delta - v_0\Delta)^2/4D\Delta}, \quad (1)$$

where v_0 is the mean molecular velocity in that pixel, D is the molecular self-diffusion coefficient and the normalizing factor A is $(4\pi D\Delta)^{-1/2}$.

The upper limit to velocity measurement in NMR is determined by the need to contain the fluid within the RF detection system and to ensure that the residence time of spins within the magnet is sufficient to achieve sufficient polarization. Both factors typically point to a maximum flow rate on the order of meters per second. The lower limit, gradient strength permitting, is determined by the competitive stochastic motion due to self-diffusion. In particular, the precision in the measurement of v_0 will be limited by the width of the distribution whose standard deviation is $(2D\Delta)^{1/2}$, and at first sight one might assign the error in v_0 as $\sqrt{2D/\Delta}$. However, in practice, the determination of the mean molecular velocity is made by locating the peak of the distribution, a process whose precision is limited by the rms noise, δP, in $\overline{P_s}(Z,\Delta)$. By taking the derivative of $\overline{P_s}(Z,\Delta)$ with respect to small deviations, δv, in velocity near the peak of the distribution, it is straightforward to show that the velocity determination error is given by

$$\delta v = \sqrt{\frac{2D}{\Delta}}\frac{\delta P}{A}, \quad (2)$$

where $A/\delta P$ is the signal-to-noise ratio in the measurement of $\overline{P_s}(Z,\Delta)$. Eq. (2) makes clear that the best velocity resolution is achieved using the longest possible encoding time Δ. In contrast, the smallest flow displacement that can be measured results from using the smallest possible Δ consistent with the requirement that the random displacements due to molecular self-diffusion do not dominate.

For small molecules, with self-diffusion coefficients on the order of $10^{-9}\,m^2\,s^{-1}$ and given encoding times limited by spin relaxation to <1 s, the lower limit to velocity measurement will be around $50\,\mu m\,s^{-1}$. For example, Holz et al. [12] reported ionic drift velocities as small as $1\times10^{-5}\,m\,s^{-1}$ measuring slow coherent flow of Li^+ ions in aqueous LiCl. In principle, given sufficient magnetic field gradient strength, the lower limit to velocity measurements could be extended considerably downwards, provided that a more slowly diffusing molecule is employed, for example, by means of a macromolecular, or molecular aggregate (micellar) tracer. However, as molecular sizes are increased, or if molecular aggregates are employed, transverse spin relaxations times tend to shorten, severely limiting the value of Δ that may be used. Another approach is to incorporate a slowly relaxing low molecular weight liquid in the interior of a larger particle, thus improving NMR visibility while retaining a slow overall diffusion coefficient of the particle.

The downward extension of velocity resolution, while intriguing in a technical sense, becomes of considerable scientific interest once the length scale of measured displacements reaches the domain of the particle size. The advantage of being able to measure small displacements at very slow velocities is that it becomes possible, in principle, to access the particle collision process, and the physics associated with the transition from ballistic to collision-dominated flow, and to do so over times sufficiently long that a broad range of experiments become possible. Feinauer et al. [13] and Altobelli et al. [14] have observed ballistic effects in granular flow, using NMR velocimetry experiments to study the flow of a liquid phase surrounded by millimeter and sub-millimeter sized solid particles. Nakagawa et al. [15–17] have studied the solid-body movement of millimeter-sized particles with liquid interiors, observing the proton NMR signal from the liquid core. In these experiments the Brownian diffusion coefficients of these granular particles is effectively zero, although flow induced dispersion effects are of course significant. In this paper, by contrast, we shall be concerned with ballistic length scale effects in aqueous colloidal suspensions, where the particle sizes are micron or submicron. In these suspensions intrinsic Brownian motion plays an important role. Nonetheless, access to the ballistic regime is in principle possible by increasing the particle size, taking advantage of converging length scales as the diffusive limit to displacement resolution drops with increasing Stokes radius. For maximum observation times of around 1 s, this regime is reached once particle diameters are on the order of 100 nm, the so-called nanoscale transition.

The problem, in NMR terms, is to find a suitably visible colloid particle of the required diameter. Again, a solid particle with a liquid core is ideal. Such a system can be readily synthesized using a simple but elegant emulsification procedure developed by Vincent and coworker [18]. With this method, particles consisting of an inner core of a high mobility oil surrounded by a solid polymer shell are obtained (see Fig. 1A), with a controllable size ranging from a few hundreds of nanometers to several microns in diameter. The core-shell particle dynamics can be observed from the NMR signal resulting from the liquid, provided that the observation time Δ is sufficiently long that the displacement of the whole particle exceeds those arising from free oil diffusion within the core. We note here that use of pulsed gradient spin echo (PGSE) NMR for probing the restricted diffusion of oil molecules inside such core-shell latex particles has been previously demonstrated by Wassenius et al. [19].

Core-shell particles are coated with an uncharged polymeric layer, which engenders a "hard sphere" character. When subjected to shear, hard-sphere colloidal dispersions exhibit complex, non-Newtonian behavior [20,21]. For example, at low volume fractions, a

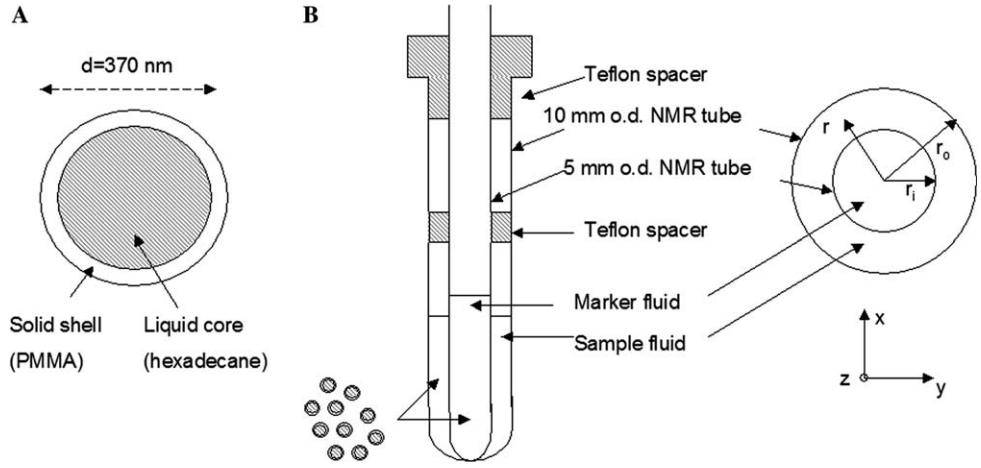

Fig. 1. (A) Composition of core-shell latex particles. (B) Sample geometry.

low-shear rate Newtonian plateau viscosity is followed by a region of shear-thinning behavior as the shear rate is increased. At increasing volume fraction, under zero-shear, a transition from the liquid state to a crystalline or a disordered, glass-like equilibrium state is observed. The solid-like behavior of concentrated colloidal systems at low shear rates is manifested through an apparent yield stress, σ_c, above which the material starts to flow with a detectable viscosity [22,23]. It has been argued that even for the solid state, weak flow will occur provided that the stress is applied for sufficient time. For such flow however the corresponding low-shear viscosity would be too high to be accurately observed in a commercial rheometer. The rheology of colloidal dispersions provides a suitable challenge for NMR velocimetry, especially if it is possible to reveal the nature of particle displacements occurring at very low velocities. The present study highlights the potential of the NMR method. In particular, we measure flow displacements for particles with a diameter of 370 nm over distances smaller than the particle size.

Note that in using such finite sized particles we must account for intra-particle diffusion effects. For the oil inside the core shell particle, diffusion is sufficiently rapid that the diffusion is completely restricted by the spherical boundaries over the diffusion time Δ, on the order of 0.5 s. For particles diffusing in spherical boundaries of radius a the apparent diffusion length is approximately $0.6a$ [7] and from the particle composition we know that the inner liquid radius is $2/3\times 185\,\text{nm} = 123\,\text{nm}$. Thus the apparent rms displacement arising from intra-molecular diffusion is 70 nm. As we will show this is much smaller than the effective particle diffusion distance, already restricted because of inter-particle collisions.

We stress that the improvement in velocity resolution reported in this article comes not specifically from improvements in NMR hardware, but rather from the choice of a suitable tracer particle. Of course, it could be argued that the ideal material for such slow velocity measurements would be a solid, for which the molecular diffusion is effectively zero. To measure slow velocities (as opposed to small displacements) one needs also to maximize the displacement encoding time. In most solid materials, the exception being some polymer networks, the relaxation times are inconveniently short. By using liquid-filled tracer particles, we optimize relaxation times, and at the same time slow the diffusion process. Coincidentally, this allows us access to an interesting domain of hard sphere particle physics.

2. Experimental

Core-shell latex particles with a liquid core of hexadecane (Aldrich H 670–3) and a solid shell of poly(methyl methacrylate) (PMMA, Acros 41,806–2500) were prepared in a 2% (w/w) aqueous dispersion of polyvinyl alcohol (PVA 95,000, Acros 18,329–5000) according to the procedure described by Loxley and Vincent [18]. The resulting dispersion of 4% (w/w) was centrifuged at 35,000 rpm in a Beckman XL-80 ultracentrifuge separating the core-shell particles from the surrounding PVA solution. The weight fraction of particles was determined by comparison of the magnitude of the CH_2 and the CH_3 peaks at 1.2 and 0.8 ppm in the ^1H NMR spectrum with the magnitude of the water peak at 4.7 ppm. From the known composition of the particles, a volume fraction of spheres, $\Phi = 46\%$ (v/v) was determined. The mean particle diameter was measured at 370 nm with low angle laser light scattering (LALLS) using a Malvern Mastersizer 2000, assigning a refractive index of 1.49 for the particles and 1.33 for the surrounding water phase.

The sample was then transferred to the Rheo-NMR cell. This comprised a 10 mm o.d. NMR tube in which is

inserted a 5 mm o.d. NMR tube, centered by two Teflon disks, as shown in Fig. 1B. This cylindrical Couette cell has a gap width d of 1.8 mm. The assembly was fitted inside a 20 mm RF coil and fixed in the microimaging probe of a Bruker AMX300 NMR system. The inner tube of the cell was rotated at a fixed frequency between 8×10^{-4} and 0.16 Hz via a drive shaft connected to a stepper motor drive system sitting on top of the magnet. Gearboxes were used to obtain high precision smooth rotation at low rotation frequencies. The sample was allowed to equilibrate for two weeks before the experiments were performed, and was not subjected to preshearing.

Velocity imaging of the sample was performed using a pulsed gradient spin echo sequence combined with Spin Warp imaging [7,8]. The pulse sequence used is shown in Fig. 2. A series of 8 separate 128×128 pixel images were obtained at different values of the PGSE encoding ("q") gradient. The displacement propagator for each pixel was obtained by Fourier transformation in the q dimension following zero-filling to 256 points. The PGSE gradient g was applied along a transverse axis x, i.e., in the flow direction (see Fig. 1), and was stepped from 0 to 0.28 T/m. δ and Δ values ranged from 1 to 15 ms and from 25 to 500 ms, respectively. Two signal averages were recorded for each q step, with a waiting time of 2 s. A representative velocity map for $f = 3.2 \times 10^{-3}$ Hz is shown in Fig. 3A with a corresponding 1D velocity profile across the map (Fig. 3B).

Note that the motion of the particles was measured by utilising the 300 MHz ^{1}H NMR signal from the hexadecane oil inside the core. To eliminate any contribution from the surrounding water to the NMR signal, the first image in each series recorded at low q was discarded from the Fourier transformation, while at higher q values the much higher water diffusion coefficient resulted in effective destruction of the water signal.

3. Results and discussion

The velocity profiles for rotational frequencies $f = 8 \times 10^{-4}$, $f = 3.2 \times 10^{-3}$, and $f = 0.16$ Hz are shown in Figs. 4A–C, corresponding to shear rates $\dot{\gamma} = 7.0 \times 10^{-3}$, $\dot{\gamma} = 0.028$, and $\dot{\gamma} = 1.40\,\mathrm{s}^{-1}$, respectively. At the lowest frequency (Fig. 4A), the velocity profile across the gap is completely flat, i.e., the whole sample moves like a solid plug. As the rotational frequency is increased, the shear stress across the gap increases, and in the inner regions of the gap the local shear stress exceeds the apparent yield stress σ_c of the sample (Fig. 4B). Whereas the outer parts of the sample are still in the solid-like state, the sample contained in the high-shear region near the inner wall now flows with a liquid-like, shear-thinning behavior. A power-law exponent n of 0.2 can be obtained from the fitting of the inner part of the velocity profile to the analytical expression for the angular velocity at radius r of a power law fluid in a wide-gap Couette geometry

$$v(r) = \omega_0 r \frac{1 - (r/r_o)^{-2/n}}{1 - (r_i/r_o)^{-2/n}} \tag{3}$$

(ω_0 = angular velocity of inner cylinder of radius r_i and r_o = radius of outer cylinder), indicating strong shear-thinning for the inner part of the fluid. At higher rotational frequencies ($f = 0.16$, Fig. 4C), the whole sample

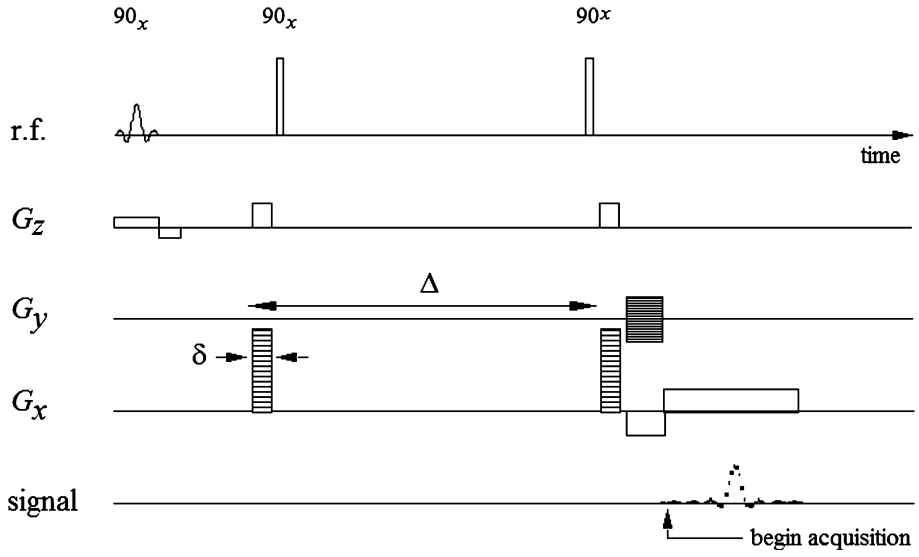

Fig. 2. Combined PGSE and spin warp pulse stimulated echo sequence for velocity encoding in the x (read) direction. Phase encoding is along the y-axis and the initial soft 90° RF pulse is used to select a slice across the Couette cell normal to the cell axis which is aligned along z. The crusher gradients in the z-direction suppress any signal contribution from the "hard" 90° RF pulses.

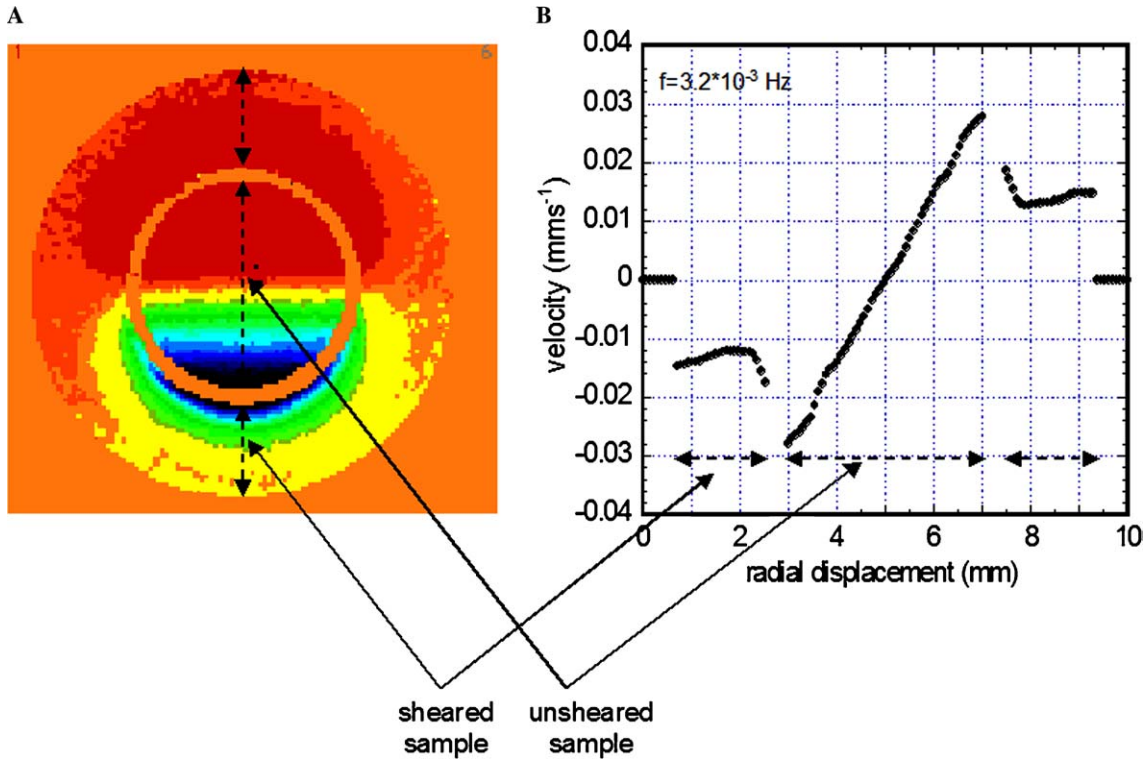

Fig. 3. (A) Velocity map of the Couette cell with the corresponding 1D velocity profile (B).

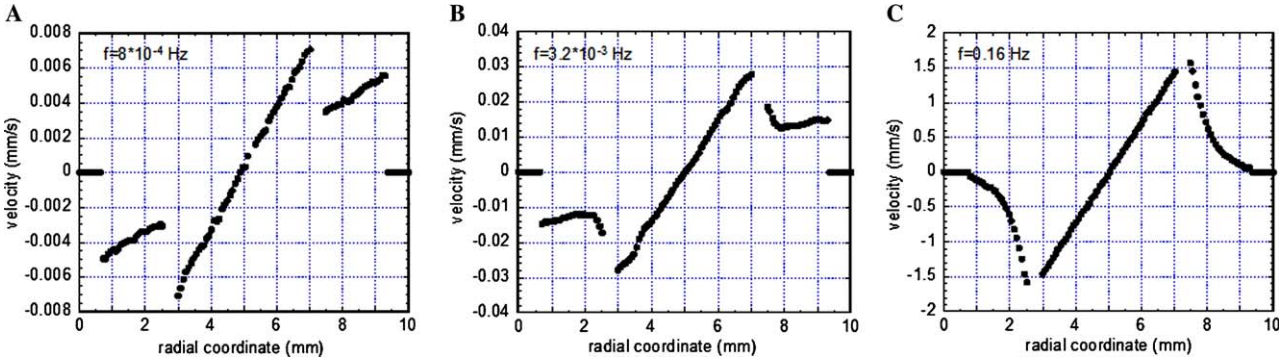

Fig. 4. (A–C) Velocity profiles for sample flowing in a Couette geometry at different rotation speeds. For the lowest rotational frequency ($f = 8 \times 10^{-4}$ Hz, A) the sample behaves like a solid plug. Note the presence of slip both at the inner and at the outer wall in (B) ($f = 3.2 \times 10^{-3}$ Hz). The inner parts of the sample have undergone a solid-to-liquid transition and flows with power-law behavior ($n = 0.2$), but the outer parts are still in a solid-like state. At higher rotational speeds ($f = 0.16$ Hz, C) the whole sample is liquid-like and shows a power-law behavior with $n = 0.4$.

is liquid-like and the shear-thinning somewhat less severe with a power law exponent n of approximately 0.4. These power law dependencies on strain rate are potentially of interest in understanding aging/rejuvenation effects in soft glassy materials and will be the subject of future work.

The observation of plug flow at the lowest rotational frequency studied ($f = 8 \times 10^{-4}$ Hz) is remarkable in that we in fact observe motion of the particles in the solid-like state of a hard-sphere colloidal system at extremely low shear rates ($\dot{\gamma} = 7.0 \times 10^{-3}\,\mathrm{s}^{-1}$). Fig. 5 shows an enlargement of the middle part of the velocity profile for $f = 8 \times 10^{-4}$ Hz, where the lowest velocity probed is on the order of $200\,\mathrm{nm\,s}^{-1}$. The velocity resolution for these measurements can be estimated from Eq. (1).

Measurement of the self-diffusion coefficient of the core-shell particles yields a value of around $2 \times 10^{-13}\,\mathrm{m}^2\,\mathrm{s}^{-1}$. Note that this corresponds to a diffusion distance of 450 nm over the encoding time of 0.5 s, around seven times the distance diffused by intra particle molecular self-diffusion alone. With a noise-to-signal ratio $\delta P/A$ of 0.014 in the NMR velocimetry measurements the minimum determination error δv for an observation time

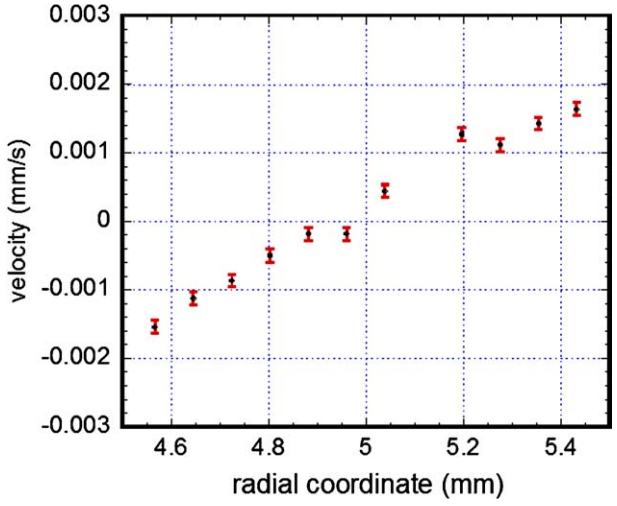

Fig. 5. Enlargement of the middle part of the velocity profile for the lowest rotational frequency, 8×10^{-4} Hz. With a noise-to-signal ratio of 0.014 in the measurement of the displacement propagator $\overline{P_s}$, the determination error in the velocity obtained from the NMR velocimetry experiments is approximately $4 \times 10^{-8}\,\mathrm{m\,s^{-1}}$, which is about half the value of the lowest velocity measured ($2 \times 10^{-7}\,\mathrm{m\,s^{-1}}$). Using an observation time Δ of 0.5 s, the lowest distance probed is thus on the order of 100 nm. The corresponding determination error in distance is approximately 50 nm, i.e., considerably smaller than the particle diameter.

Δ of 0.5 s is $100\,\mathrm{nm\,s^{-1}}$, corresponding to an error in the probed distance $v\Delta$ of approximately 50 nm. Note that Eq. (2) shows that it is possible to resolve the flow displacement to a somewhat smaller distance than the rms displacement due to diffusion alone. The velocity resolution is comparable with the lowest velocity measured, and the displacement resolution is considerably smaller than the particle diameter. We are thus able to accurately probe displacements comparable with the particle diameter.

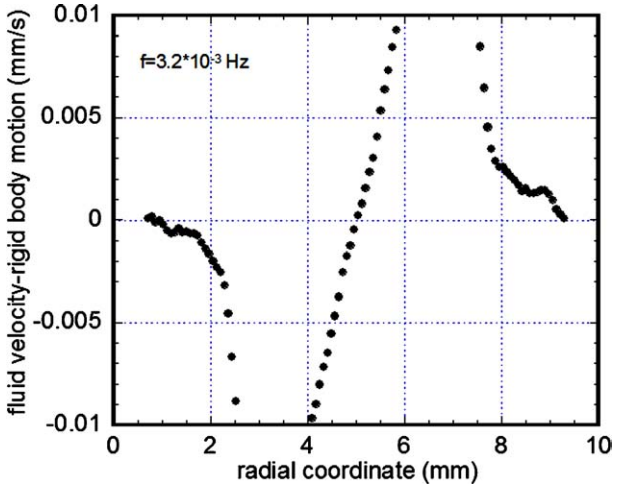

Fig. 6. Enlargement of the gap part of the velocity profile for the rotational frequency, 3.2×10^{-3} Hz, in which the background rigid body motion has been subtracted, revealing the local shear flow. Flow relative to the background rigid body motion is resolved to an error of ±50 nm.

To emphasise that we are not only able to resolve the very slow "rigid body" motion of the central cylinder, we show, in Fig. 6, the velocity across the couette cell, relative to the background rigid body motion, i.e., $v(r) - \omega r$, where ω is the angular velocity of the fluid as measured at the outer wall. We have chosen for this data, the rotation speed of 0.0032 Hz, for which non-rigid body deformational flow is present near the inner all. This figure reveals the local shearing flow and shows that we are equally able to measure such relative flow at very small velocities.

4. Conclusions

In flow, displacements due to the local fluid velocity are superposed on displacements due to Brownian motion. We have shown that, by employing a sufficiently slowly diffusing tracer particle, the NMR velocimetry technique can be extended down to the nanoscale domain. Interestingly, the smallest flow displacement that can be measured is not the rms displacement due to diffusion, but may be considerably smaller if the signal-to-noise ratio is sufficiently high. By the use of NMR-visible, core-shell particles, distances down to a few hundreds of nanometers have been probed, allowing the observation of the solid-to-liquid transition of a concentrated colloidal system. Remarkably, we are able to observe sub-diameter displacements over a timescale as long as 0.5 s. Nonetheless, these displacements are still larger than the collision distance because of the close packing of the particles in our high volume fraction colloid. By reducing Δ, we can, in principle, cross the ballistic to collisional transition, although at this point, the Brownian motion of the particles will increase to the free Stokesian value as the effects of restricted diffusion disappear. We intend to use the Rheo-NMR method outlined here to probe such behavior, and to observe the transient effects of flow startup and cessation. By this means we hope to explore new possibilities for NMR velocimetry as an experimental tool for colloidal chemistry and physics.

Acknowledgments

H.W. acknowledges financial support from BIM Kemi AB and from KIF AB (The Research School of the Swedish Chemical Industry) for the Ph.D. project and from Chalmers University of Technology for the sabbatical visit to New Zealand. P.T.C. acknowledges support form the Royal Society of New Zealand Marsden Fund, the Centres of Research Excellence Fund and the New Zealand Foundation for Research, Science and Technology.

References

[1] E.L. Hahn, Spin echoes, Phys. Rev. 80 (4) (1950) 580–594.

[2] H.Y. Carr, E.M. Purcell, Effects on diffusion on free precession in nuclear magnetic resonance experiments, Phys. Rev. 94 (3) (1954) 630–638.

[3] E.O. Stejskal, J.E. Tanner, Spin diffusion measurements: spin echoes in the presence of a time-dependent field gradient, J. Chem. Phys. 42 (1) (1965) 288–292.

[4] R.J. Hayward, D.J. Tomlinson, K.J. Packer, Pulsed field-gradient spin-echo NMR studies of flow in fluids, Mol. Phys. 23 (6) (1972) 1083–1102.

[5] L.F. Gladden, P. Alexander, Applications of nuclear magnetic resonance imaging in process engineering, Meas. Sci. Technol. 7 (1996) 423–435.

[6] P. Griffiths, N. Hoggard, W. Dannels, I. Wilkinson, In vivo measurements of cerebral blood flow: a review of methods and applications, Vasc. Med. 6 (1) (2001) 51–60.

[7] P.T. Callaghan, Principles of Nuclear Magnetic Resonance, Oxford University Press, Oxford/New York, 1991.

[8] P.T. Callaghan, Y. Xia, Velocity and diffusion imaging in dynamic NMR microscopy, J. Magn. Reson. 91 (1991) 326–352.

[9] P.T. Callaghan, Rheo-NMR: nuclear magnetic resonance and the rheology of complex fluids, Rep. Prog. Phys. 62 (1999) 599–670.

[10] A. Caprihan, E. Fukushima, Flow measurements by NMR, Phys. Rep. 198 (1990) 195–235.

[11] E. Fukushima, Nuclear magnetic resonance as a tool to study flow, Annu. Rev. Fluid Mech. 31 (1999) 95–123.

[12] M. Holz, C. Müller, A.M. Wachterm, Modification of the pulsed magnetic field gradient method for the determination of low velocities by NMR, J. Magn. Reson. 69 (1986) 108–115.

[13] A. Feinauer, S.A. Altobelli, E. Fukushima, NMR measurements of flow profiles in a coarse bed of packed spheres, Magn. Reson. Imaging 15 (1997) 479–487.

[14] S.A. Altobelli, E. Fukushima, L.A. Mondy, Nuclear magnetic resonance imaging of particle migration in suspensions undergoing extrusion, J. Rheol. 41 (1997) 1105–1115.

[15] M. Nakagawa, S.A. Altobelli, A. Caprihan, E. Fukushima, E. Jeong, Non-invasive measurements of granular flows by magnetic resonance imaging, Exp. Fluids 16 (1993) 54–60.

[16] M. Nakagawa, S.A. Altobelli, A. Caprihan, E. Fukushima, NMR measurement and approximate derivation of the velocity depth-profile of granular flow in a rotating, partially filled, horizontal cylinder, Powders and Grains 97, in: Proceedings of the 3rd International Conference on Powders and Grains, Balkema, Rotterdam, Netherlands, 1997.

[17] M. Nakagawa, S.A. Altobelli, A. Caprihan, E. Fukushima, NMRI study: axial migration of radially segregated core of granular mixtures in a horizontal rotating cylinder, Chem. Eng. Sci. 52 (1997) 4423–4428.

[18] A. Loxley, B. Vincent, Preparation of core-shell latex particles, J. Colloid Interface Sci. 208 (1998) 49.

[19] H. Wassenius, M. Nydén, B. Vincent, NMR diffusion studies of translational properties of oil inside core-shell latex particles, J. Colloid Interface Sci. 264 (2003) 538–547.

[20] R.G. Larson, The Structure and Rheology of Complex Fluids, Oxford University Press, Oxford, New York, 1999.

[21] W.B. Russel, D.A. Saville, W.R. Schowalter, Colloidal Dispersions, Cambridge University Press, Cambridge, 1989.

[22] C.G. De Kruif, E.M.F. van Iersel, A. Vrij, W.B. Russel, Hard sphere colloidal dispersions: viscosity as a function of shear rate and volume fraction, J. Chem. Phys. 83 (1985) 4717.

[23] D.A.R. Jones, B. Leary, D.V. Boger, The rheology of a concentrated colloidal suspension of hard spheres, J. Colloid Interface Sci. 147 (2) (1991) 479–495.